

Light-induced defects in hydrogenated amorphous silicon studied by the constant-photocurrent method

J. A. Schmidt,* R. Arce, R. H. Buitrago,[†] and R. R. Koropecski[‡]

Instituto de Desarrollo Tecnológico para la Industria Química, UNL-CONICET, Güemes 3450, 3000 Santa Fe, Argentina

(Received 23 July 1996)

The light-induced creation of metastable defects in undoped hydrogenated amorphous silicon has been followed using photoconductivity and absorption coefficient measurements. The density of states in the gap was obtained from the deconvolution of the subgap absorption coefficient measured by the constant-photocurrent method. We found that the decay of the photoconductivity and the evolution of the integrated density of subgap states follow the dependence on illumination time (t_{ill}) predicted by the “bond-breaking” model. The density of occupied states obtained from the deconvolution procedure shows the presence of two peaks within the gap. After subtracting the valence band-tail contribution, these peaks can be well fitted with two Gaussians. The areas of both Gaussians increase as $t_{\text{ill}}^{1/3}$ while their positions and widths remain unchanged. According to the energy position of these peaks, they are ascribed to the neutral and negatively charged silicon dangling bonds D^0 and D^- . We found that in this intrinsic sample the density of charged defects exceeds that of neutral defects, their ratio D^-/D^0 being approximately 2.6. This ratio is independent of the illumination time. [S0163-1829(97)02911-1]

I. INTRODUCTION

The creation of a large number of metastable defects during illumination (the Staebler-Wronski effect¹) is a serious drawback for the widespread use of hydrogenated amorphous silicon (a -Si:H) in solar cells and other electronic devices. The increase in the density of defects leads to a decay of the photoconductivity (σ_{ph}) with the illumination time (t_{ill}). The evolution of σ_{ph} with t_{ill} is frequently used as a quick estimate of the stability of a given a -Si:H sample.^{2,3} Electron spin resonance (ESR) has been extensively used to measure the increase of the defect density upon illumination.⁴⁻⁶ As ESR detects paramagnetic centers, it is only sensitive to the density of neutral silicon dangling bonds. It has been traditionally assumed that the density of neutral defects largely exceeds the density of charged defects in undoped a -Si:H. If this were the case, this would allow us to use the spin density as an indication of the total density of defects. However, some recent works⁷⁻¹² have suggested the presence of many charged defects even in undoped samples, both in the annealed and light-soaked states. These works are both theoretical,^{9,10} based on the defect pool model, and experimental, based on ESR-photothermal deflection spectroscopy comparisons^{7,8} and on light-induced ESR (LESr) measurements.^{11,12} However, other LESr (Ref. 13) and modulated ESR (Ref. 14) measurements seem to indicate a larger density of neutral defects than charged defects. Thus it seems desirable that another reliable method should be used to measure the densities of the different charged states of the silicon dangling bond. Such a method would also be very suitable for following the kinetics of defect creation under illumination for the different defects.

The density of states (DOS) within the gap of a -Si:H determines the optical properties of the material. Thus an appropriate deconvolution of the sub-band-gap absorption coefficient (α) can be used to obtain the DOS. Among the

methods proposed to measure α as a function of energy, the constant-photocurrent method¹⁵ (CPM) seems to be very suitable because of its experimental simplicity and its sensitivity to bulk states.¹⁶ Although it has limitations,¹⁷ the CPM is widely used for determining $\alpha(E)$. In order to obtain the DOS from the $\alpha(E)$ data, two approaches can be made. One is to model the distribution of gap states with a function having some free parameters,¹⁸⁻²⁰ which are determined from a fitting to the experimental spectra. This is usually done by assuming the presence of one, two, or three Gaussian functions within the gap, whose area, position, and width are obtained from the fitting. The other approach is to apply an appropriate deconvolution technique to the $\alpha(E)$ data, as discussed in previous works.²¹⁻²³ We have followed this second approach, details of which are given in Sec. III.

In this paper we use the deconvolution of CPM spectra to obtain the occupied density of subgap states. This shows that two defect bands exist between the midgap and the valence band. Based on the energy position of these defects, we assign them to the neutral dangling bonds D^0 and the negatively charged dangling bonds D^- . We study the dependence on illumination time of the density of both defect states. We also measure the photoconductivity decay, comparing this result with the evolution of the density of defects and the predictions of existing models.

II. EXPERIMENTAL PROCEDURES

Samples were deposited onto Corning 7059 glass in a conventional parallel-plate capacitively coupled plasma-enhanced chemical vapor deposition reactor operated at 13.56 MHz. Pure silane was introduced in the reactor at a flow rate of 40 SCCM (where SCCM denotes cubic centimeter per minute at STP). The substrate was fixed to the grounded electrode and its temperature was kept at 210 °C. The pressure in the chamber was 920 μ bars and the rf power density was 20 mW/cm². Under these conditions the deposition rate was 2 Å/s. For this study we have grown a sample

860 nm thick. The film thickness was measured from the UV-visible transmittance spectrum, using interference techniques.²⁴ The absorption coefficient in the strong absorption region was also evaluated from the UV-visible spectrum.

Two silver strips (1.5 mm long, separated by a gap of 0.25 mm) were evaporated on the sample as contacts. Conductivity measurements were done in a cryostat under vacuum conditions (better than 10^{-6} Torr). Dark conductivity was measured in the initial (annealed) and final (fully-light-soaked) state as a function of temperature, while the sample was cooled at a rate of 2 °C/min. The initial state was obtained by annealing the as-deposited sample for two hours at 180 °C. When measuring the light-soaked state the temperature was kept below 80 °C to avoid thermal annealing. The dark conductivity activation energy was extracted from the temperature range between 300 and 340 K for both states.

The degradation experiments were performed using monochromatic light from a He-Ne laser ($\lambda = 632.8$ nm, $h\nu = 1.96$ eV) with an intensity of 32 mW/cm². The generation rate (G) was 6.3×10^{20} cm⁻³ s⁻¹, as obtained from the formula given by Seeger²⁵ for non-uniform absorption. The photoconductivity decay was measured while the sample was illuminated with the laser.

The subgap absorption coefficient (α) was obtained by means of the dc constant photocurrent method. The measurement was performed at room temperature. We used a double monochromator system and the photocurrent was kept constant by controlling the intensity of the incident light by means of a computer program. The absolute values of α were obtained by matching the CPM data to the results of conventional optical measurements at 1.8 eV. We took CPM spectra after the following illumination times: 0, 180, 780, 1980, 9180, and 23 580 s. Measurements of the CPM spectra and the photoconductivity decay were performed without changing the position of the sample in the cryostat. The suppression of the interference pattern from the CPM spectra was done using the transmittance spectra,²⁶ followed by a final smoothing using fast Fourier transform filtering. All spectra were treated in the same way, taking into account the comparative nature of this study.

III. RESULTS

We measured the temperature dependence of the dark conductivity in the initial (annealed) and final (light soaked for 23 580 s) state. The low-temperature activation energy of the dark conductivity curves evolved from 0.81 eV in the initial state up to 0.88 eV in the final state, while the room-temperature dark conductivity decreased from 2×10^{-10} to 5×10^{-11} Ω^{-1} cm⁻¹.

We monitored the photoconductivity decay as the sample was degraded with the laser light. A plot of photoconductivity versus illumination time on logarithmic scales showed a $-1/3$ slope for long illumination times. This is indicative that the photoconductivity decay follows the law predicted by the bond-breaking model:^{27,28}

$$[\sigma_{\text{ph}}(t_{\text{ill}})]^{-3} - [\sigma_{\text{ph}}(0)]^{-3} = Pt_{\text{ill}}. \quad (1)$$

In Fig. 1 the photoconductivity data have been plotted according to Eq. (1). A linear fit of the data gives a slope

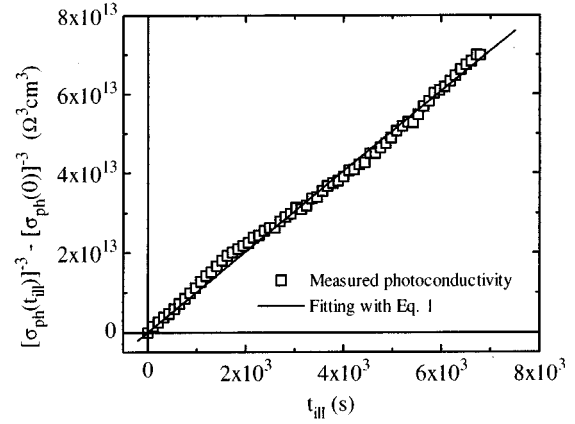


FIG. 1. Photoconductivity decay as a function of illumination time, plotted according to the bond-breaking model [Eq. (1)]. The full line, whose slope is $P = (2.0 \pm 0.5) \times 10^{10}$ Ω^3 cm³/s, corresponds to a linear fit.

$P = (2.0 \pm 0.5) \times 10^{10}$ Ω^3 cm³/s. Although some of its assumptions have been questioned,²⁹ the model proposed by Stutzmann, Jackson, and Tsai (SJT)²⁸ describes accurately the observed kinetics of defect creation, so we will use it in this work. According to this model, P is determined from

$$P = \frac{3 C_{\text{SW}} A_t}{A_n A_p B^3 G}, \quad (2)$$

where A_n and A_p are effective transition probabilities between tail and defect states for electrons and holes, respectively, A_t is the transition probability for tail-to-tail recombination, C_{SW} is the average efficiency of defect creation by tail-to-tail transitions, G is the generation rate, and $B = e[\mu_n/A_n + \mu_p/A_p]$ (e being the electron charge and μ_n, μ_p the average mobilities for electrons and holes, respectively). Taking for A_n and A_p the values given by SJT and for μ_n and μ_p typical values of 10 and 1 cm²/V s respectively,³⁰ we get $C_{\text{SW}} A_t = 2.3 \times 10^{-15}$ cm³ s⁻¹ from Eq. (2). This result can be compared with the independent measurement of the evolution of the defect density with the illumination time as follows.

From the CPM measurements (Fig. 2) we observed a steady increase of the absorption coefficient in the subgap region as the sample was degraded, while the Urbach tail remained unchanged. In order to get a quick estimate of the evolution of the integrated defect density (N_d), we used two different approaches. Both procedures implicitly assume that the defects are homogeneously distributed throughout the sample. One approach was to integrate the excess subgap absorption (subtracting the contribution from the Urbach tail) using the formula:¹⁶

$$N_d = 1.9 \times 10^{16} \int (\alpha - \alpha_{\text{Urbach}}) dE. \quad (3)$$

The other method was to use the value of the absorption coefficient at 1.2 eV, assuming that $\alpha(1.2 \text{ eV}) = 1 \text{ cm}^{-1}$ corresponds to $N_d = 2.5 \times 10^{16}$ cm⁻³ defect states^{31,32} and that the relation is linear. The difference between the results from both methods was less than 50%. In Fig. 3 we show the evolution with the illumination time of the defect density

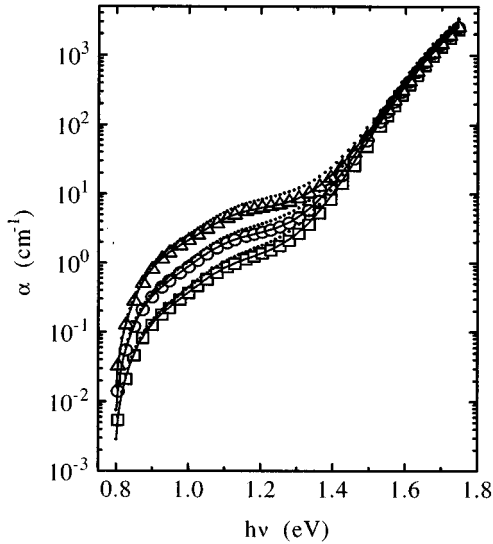


FIG. 2. Absorption coefficient for different illumination times: 180 s (\square), 1980 s (\circ), and 23 580 s (Δ). The lines correspond to the convolution [using Eq. (6)] of the densities of states obtained by deconvoluting the measured $\alpha(E)$ data with Jensen's method (Refs. 23) (—) and deconvoluting the measured $\alpha(E)$ data with the derivative method (Refs. 21 and 22) (---).

measured by both methods. The $\log(N_d)$ vs $\log(t_{\text{ill}})$ plot shows a linear behavior with a slope very close to 1/3 in both cases. This allows us to fit the evolution of the defect density with the bond-breaking formula.²⁸

$$[N_d(t_{\text{ill}})]^3 - [N_d(0)]^3 = Ct_{\text{ill}}, \quad (4)$$

which gives $C = 7.8 \times 10^{44} \text{ cm}^{-3} \text{ s}^{-1}$ from Eq. (3) and $C = 2.4 \times 10^{45} \text{ cm}^{-3} \text{ s}^{-1}$ from $\alpha(1.2 \text{ eV})$. Within the frame of SJT's model,²⁸ the constant C is related to the $C_{\text{SW}}A_t$ product by

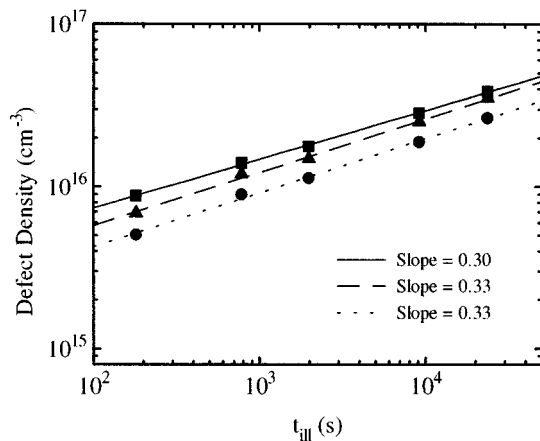


FIG. 3. Evolution of the integrated defect density with illumination time, as measured from the absorption coefficient at 1.2 eV, (\blacksquare) the integrated excess absorption coefficient (\bullet), and the deconvoluted density of states (\blacktriangle) (see the text). The lines correspond to linear fits. The three slopes are very close to the 1/3 value predicted by the bond-breaking model.

$$C_{\text{SW}}A_t = \frac{A_n A_p C}{3G^2}, \quad (5)$$

where the parameters have the same meaning as in Eq. (2). Using the values previously adopted for A_n and A_p , and the values of C obtained from Eq. (4), we get $C_{\text{SW}}A_t = 1.4 \times 10^{-15} \text{ cm}^3 \text{ s}^{-1}$ from Eq. (3) and $C_{\text{SW}}A_t = 4.3 \times 10^{-15} \text{ cm}^3 \text{ s}^{-1}$ from $\alpha(1.2 \text{ eV})$. These values coincide fairly well with the one obtained from the photoconductivity decay [Eq. (2)] and are also comparable with other results given in the literature, like the $C_{\text{SW}}A_t$ product measured by SJT (Ref. 28) ($1.5 \times 10^{-15} \text{ cm}^3 \text{ s}^{-1}$).

The absorption coefficient measured by the CPM can be written as^{31,33}

$$\alpha(E) = \frac{KP^2(E)}{E} \int_{-\infty}^{\infty} g_i(\varepsilon) f(\varepsilon) g_f(\varepsilon + E) [1 - f(\varepsilon + E)] d\varepsilon, \quad (6)$$

where g_i and g_f are the densities of initial and final states for the optical transitions, respectively, f is the proper statistical occupation function, E is the photon energy, and K is a constant. It is usually assumed that the matrix elements for the optical transitions $P^2(E)$ are constant. We have taken³³ $[KP^2(E)] = 4.34 \times 10^{-38} \text{ cm}^5 \text{ eV}^2$. In the CPM technique, only transitions contributing to the photoconductivity are detected. Some authors^{34,35} have argued that conduction tail states may contribute to the photocurrent. However, the most common assumption is to consider only transitions leading to the excitation of carriers into extended states.^{21,22,31,33} This implies that the lower limit of the integral in Eq. (6) is $(E_c - E)$, where E_c is the conduction-band mobility edge. Assuming that $g_f(E)$ is constant above E_c and $[1 - f(\varepsilon + E)] \approx 1$, the density of filled states $[g_i(E)f(E)]$ can be evaluated in a simple way by differentiation of the $\alpha(E)$ spectrum. This is the derivative method, used by Pierz, Mell, and Terukov²¹ and Amato, Giorgis, and Spagnolo.²² However, $g_f(E)$ is thought to vary as $E^{1/2}$ above E_c . Jensen²³ introduced a correction to the derivative method that allows the accurate determination of the DOS assuming a parabolic energy dependence for $g_f(E)$. We used this method to deconvolute our $\alpha(E)$ data (assuming, as before, that the defects are homogeneously distributed throughout the sample). The resulting DOS is shown in Fig. 4. It can be seen that, as t_{ill} increases, two peaks grow in the midgap region, while the valence-band tail remains practically unchanged. This is one of the first observations of the presence of two peaks between the valence band and the Fermi energy in a -Si:H. In a previous work, Sakata *et al.*¹⁹ found two distinct defect states in the lower midgap of undoped a -Si:H. They also used deconvolution of CPM measurements, but the deconvolution was performed by fitting a proposed model for the DOS. Günes, Wronski, and McMahon²⁰ also found two peaks in the lower half of the gap when applying a fitting procedure to deconvolute their dual beam photoconductivity data. It is worthwhile noting that the deconvolution procedure we have used does not assume any special shape for the DOS, so it represents a direct observation of the presence of two distinct defect states. The valence-band-tail states extend exponentially into the gap. By subtracting the contributions of these states, we get the evolution of the mid-

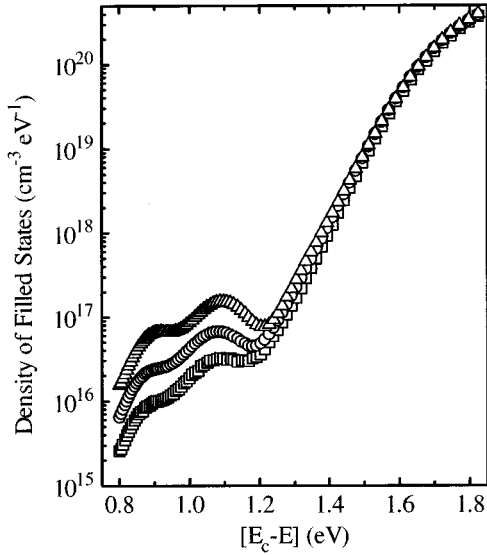


FIG. 4. Density of filled states, obtained from the deconvolution of the absorption coefficient data, for different illumination times: 180 s (□), 1980 s (○), 23580 s (Δ). Two peaks are present in the subgap region that grow as the sample is degraded. The valence-band-tail states, on the other hand, remain practically unchanged.

gap DOS with the subsequent degradation of the sample. As can be seen in Fig. 5, the occupied density of defect states consists of two (apparently) Gaussian peaks that evolve as a function of illumination time. The Gaussian shape is commonly assumed to describe the defect density and it comes from a statistical energy distribution for the defect sites. In accordance with Sakata *et al.*,¹⁹ we fit the evolution of the peaks with Gaussians of constant position and width. This is so because we do not expect any change in the nature of the defect states produced by light soaking. The best fit for the complete set of curves was obtained with peak energy positions at 0.91 ± 0.01 and 1.090 ± 0.008 eV from the

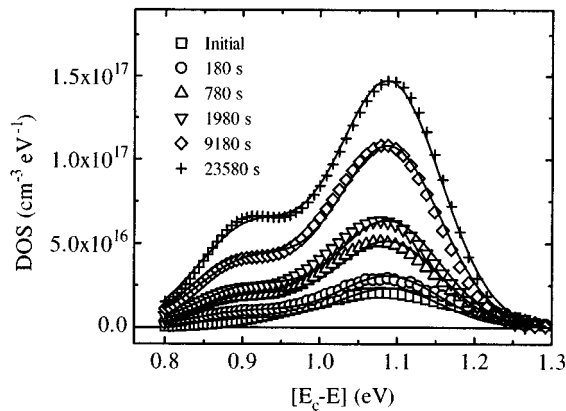


FIG. 5. Evolution of the density of midgap states with illumination time once the contribution from the valence-band-tail states has been subtracted. The peaks are fitted with two Gaussians (full lines), centered at 0.91 and 1.09 eV from the conduction-band mobility edge. The areas of both Gaussians tend to increase when the sample is degraded. The width of the Gaussians is fixed at 0.14 eV.

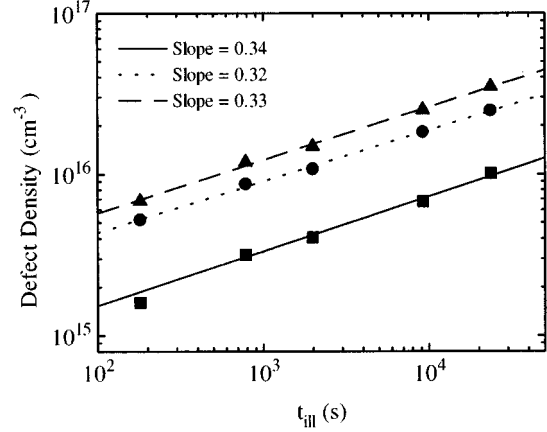


FIG. 6. Evolution of the density of subgap states as a function of illumination time. Shown are the area of the low-energy Gaussian peak from Fig. 5, (■), the area of the high-energy Gaussian peak, (●), and the resultant density of defects when the areas of both Gaussians are added up (▲). The lines correspond to linear fits (the data points included in the fitting are those for which the density of defects is at least two times larger than the initial density of defects).

conduction-band edge, being the width 0.14 ± 0.02 eV in both cases. The areas of both peaks tend to increase monotonically as a function of illumination time, as shown in Fig. 6. It can be seen that the evolution of the area of each peak has a dependence on t_{ill} very close to $t_{\text{ill}}^{1/3}$ in the long-time limit (once the density of defects exceeds the initial defect density by a factor of 2 or more). When the areas of the two Gaussians are added up, the total defect density also grows as $t_{\text{ill}}^{1/3}$, in accordance with the results obtained from $\alpha(1.2$ eV) and Eq. (3) (see also Fig. 3). Equation (4) was also used to fit the evolution of the total defect density obtained from the deconvolution, obtaining $C = 1.6 \times 10^{45} \text{ cm}^{-3} \text{ s}^{-1}$. From Eq. (5), and using the values previously adopted for A_n and A_p , we get $C_{SW}A_t = 2.9 \times 10^{-15} \text{ cm}^3 \text{ s}^{-1}$. This value is in between those obtained from Eq. (3) and $\alpha(1.2$ eV) and it is also in excellent agreement with the $C_{SW}A_t$ product obtained from the photoconductivity decay.

IV. DISCUSSION

In the first place, it is essential to be sure that the deconvolution procedure that we applied yields valid estimates of the deep level density. In order to test the accuracy of the method, we did the following: starting from the densities of states obtained from the deconvolution (Fig. 4), we applied Eq. (6) to generate the $\alpha(E)$ spectra. These were in excellent agreement when compared with the measured $\alpha(E)$ data (see Fig. 2). This gave us an indication of the self-consistency of the method. We also verified that a purely derivative method (like those of Refs. 21 and 22) does not reproduce the original $\alpha(E)$ data (as shown in Fig. 2). The accuracy of the method that we have applied for reproducing a previously assumed DOS has also been verified by Jensen in Ref. 23.

As it can be observed from Figs. 1 and 3, both the photoconductivity decay and the evolution of the defect density follow the dependence on illumination time predicted by the

bond-breaking model. We used three methods to obtain the density of gap states (N_d) in this sample: from $\alpha(1.2 \text{ eV})$ we obtained $N_d^{\alpha(1.2 \text{ eV})}$, from Eq. (3) we obtained $N_d^{f\Delta\alpha dE}$, and from the deconvolution we obtained N_d^{dec} . The densities of states obtained from all these methods are in fairly good agreement within the experimental error and they all give the predicted $t_{\text{ill}}^{1/3}$ dependence. $N_d^{\alpha(1.2 \text{ eV})}$ is greater than N_d^{dec} , while $N_d^{f\Delta\alpha dE}$ is smaller than N_d^{dec} . The calibration constant used to get $N_d^{f\Delta\alpha dE}$ from Eq. (3) was obtained by Smith *et al.*¹⁶ by comparing their CPM measurements with ESR determinations. As ESR measures paramagnetic defects, it detects only neutral silicon dangling bonds and does not “see” charged defects. Thus it is not unexpected that $N_d^{f\Delta\alpha dE}$ is smaller than N_d^{dec} since the latter measures the density of D^0 and D^- states. The constant applied to relate $\alpha(1.2 \text{ eV})$, with $N_d^{\alpha(1.2 \text{ eV})}$ has been obtained recently by Siebke and Stiebig,³² who used total-yield photoelectron spectroscopy (TYPES) to measure the defect density of *a*-Si:H samples. As TYPES detects the occupied density of states regardless of their charge state, it would be expected that $N_d^{\text{dec}} \approx N_d^{\alpha(1.2 \text{ eV})}$. This is not the case for our sample. However, it should be noted that there is a certain dispersion in the values reported by different authors for the calibration constant (in the range from 1×10^{16} to $5 \times 10^{16} \text{ cm}^{-3}$; see Ref. 31 and references therein).

The value obtained for $C_{\text{sw}}A_t$ from the photoconductivity decay ($2.3 \times 10^{-15} \text{ cm}^3 \text{ s}^{-1}$) coincides reasonably well with those obtained from the evolution of N_d (4.3×10^{-15} , 1.4×10^{-15} , and $2.9 \times 10^{-15} \text{ cm}^3 \text{ s}^{-1}$ from $N_d^{\alpha(1.2 \text{ eV})}$, $N_d^{f\Delta\alpha dE}$, and N_d^{dec} , respectively). The photoconductivity decay is measured in a simpler and faster way than the evolution of the defect density, but the values of $C_{\text{sw}}A_t$ obtained from σ_{ph} are affected by the uncertainty in the values of the mobilities [which enter to the third power in Eq. (2)]. As these average mobilities depend mainly on the band states, they should not be affected by changes in the subgap density of states. However, it should be of importance to verify this assumption, studying the behavior of μ_n and μ_p while the sample is degraded.

A large number of experiments^{36–39} have shown that the density of states in the gap of *a*-Si:H is dominated by the three different charge states of the silicon dangling bond: D^0 , D^+ , and D^- . The position of the low-energy peak in Fig. 5 is very close to the center of the gap. From Fig. 6 it can also be seen that it grows as $t_{\text{ill}}^{1/3}$, which is the time dependence of the density of neutral silicon dangling bonds (as measured by ESR). According to this, we ascribe the peak centered at $\sim(E_c - 0.91 \text{ eV})$ to the neutral dangling bonds D^0 . The other peak is shifted by 0.18 eV towards the valence band, and we ascribe it to the negatively charged defects D^- . These assignments are consistent with the energy distribution of the defects proposed by the potential fluctuations,⁴⁰ defect pool,^{9,10} and thermodynamic equilibrium⁴¹ models. Sakata *et al.*¹⁹ obtained the best fit of their $\alpha(E)$ data placing two Gaussian peaks at $E_c - 1.0$ and $E_c - 1.1 \text{ eV}$, with half-widths of 0.15 and 0.08 eV, respectively. These same positions and widths were used in the annealed and light-soaked states. On the other hand, Günes, Wronski, and McMahon²⁰ allowed a change in the half-width of the D^- peak for the light-soaked state. They ob-

tained the following parameters: positions $0.78 \text{ eV} - E_v$ and $0.50 \text{ eV} - E_v$ and half-widths 0.13 and 0.08 eV in the annealed state and 0.13 and 0.12 eV in the light-soaked state. As they assumed a mobility gap of 1.9 eV, the positions of the peaks relative to the conduction-band mobility edge would be $E_c - 1.12$ and $E_c - 1.4 \text{ eV}$, respectively. As it can be seen, there is a relatively high dispersion in the values of the peaks positions reported by these authors. The D^- peak position obtained by Günes, Wronski, and McMahon²⁰ is within the valence-band tail, so it would be difficult to extract it from a deconvolution procedure. On the other hand, the D^0 peak position is not at the center of the gap. The peaks positions obtained by Sakata *et al.*¹⁹ are closer to our findings. Whereas the method used by these authors assumes a particular shape for the density of states in the gap, our method leads to similar results without that *a priori* assumption. When fitting our results, we kept fixed the centers and the widths of the Gaussians. We adjusted the whole series of data with only the areas of the Gaussians varying as a function of light-soaking time. From Fig. 5 it can be observed that the fitting is very good in spite of the small number of free parameters.

The density of charged defects in intrinsic *a*-Si:H is a controversial topic. While some authors agree with the traditional point of view that the density of neutral defects largely exceeds the density of charged defects,^{13,14} other authors maintain the opposite opinion.^{8–10} However, an increasing amount of recent observations^{7,8,11,12} tend to confirm that the density of charged defects is not negligible in intrinsic *a*-Si:H. Our results agree with these later measurements since the ratio of the areas of the D^-/D^0 peaks (as obtained from the Gaussians of Fig. 5) is approximately equal to 2.6. Sakata *et al.*¹⁹ also obtained a density of charged defects higher than the density of neutral defects by a factor of 3–5, at least for their initial state. When illuminated, their samples showed a decrease in the density of D^- , while the D^0 density increased. Other authors^{8–10,42} have also claimed that illumination creates mainly D^0 states, thus leading to a disproportionality in the spin versus total defect density. If this were true, and if the density of charged defects were comparable to the neutral defect density, then the bond-breaking model proposed by SJT (Ref. 28) would contradict the ESR measurements. There is considerable experimental evidence from ESR (Refs. 28 and 43) showing that the spin density grows as $t_{\text{ill}}^{1/3}$. Thus, if it were true that the D^0 density grows faster than the density of charged defects, then the total defect density would grow with a smaller dependence on t_{ill} . This would be in disagreement with the bond-breaking model, which predicts a $t_{\text{ill}}^{1/3}$ dependence for the total density of defects. However, our measurements show that the densities of the D^0 and D^- levels grow at the same rate (Fig. 6). We have found a proportionality between the density of charged and neutral defects, which remains for the different light-soaked states (except for the initial state, where the determination of the density of D^0 states is affected by a large uncertainty). This implies that the bond-breaking model is applicable, even when there are more charged than neutral defects.

V. CONCLUSION

In this paper we have studied the light-induced degradation of an *a*-Si:H sample by means of the photoconductivity

decay and the evolution of the subgap absorption coefficient measured by the CPM. The deconvolution of the $\alpha(E)$ data allowed us to obtain the occupied density of states without any *a priori* assumption on its shape. The DOS showed the presence of two peaks between the valence band and the Fermi energy. After subtracting the valence-band-tail contribution, these peaks have been fitted with Gaussians of constant positions and widths, whose areas increased as a function of illumination time. We have assigned the midgap peak to the neutral dangling bonds D^0 and the peak closer to the valence band to the negatively charged defects D^- . We have found that the D^- density is greater than D^0 density, which is the prediction of the defect pool model. We have also found that the densities of both defects grow as $t_{\text{ill}}^{1/3}$. This is in agreement with ESR measurements, which show a spin density growing with the same time dependence. It also verifies that the spin density is proportional to the total density of defects, an assumption that has been questioned lately. The proportionality between D^0 and D^{tot} makes SJT's (Ref. 28)

model applicable even when there are more charged than neutral defects.

The evolution of the photoconductivity as a function of illumination time also follows the bond-breaking model. The parameters that we have obtained from the evolution of N_d , whether measured from $\alpha(1.2 \text{ eV})$, from Eq. (3), or from the deconvoluted DOS, agree reasonably well with those found from the photoconductivity decay. This agreement strengthens the confidence in the results of our present work.

ACKNOWLEDGMENTS

The authors thank M. Passeggi, A. Gennaro, and E. Albanesi for critical readings of the manuscript. This work was partially supported by the OEA (Project "Programa Multinacional de Materiales") and the CONICET (Project No. BID 236).

*Electronic address: jschmidt@intec.unl.edu.ar

†Also at Departamento de Física, Facultad de Ingeniería Química, Universidad Nacional del Litoral, Santiago del Estero 2829, 3000 Santa Fe, Argentina.

¹D. L. Staebler and C. R. Wronski, *Appl. Phys. Lett.* **31**, 292 (1977).

²J. Xi, J. Macneil, T. Liu, and M. Gosh, *Appl. Phys. Lett.* **60**, 1975 (1992).

³J. A. Schmidt, R. R. Koropecski, R. Arce, and R. H. Buitrago, *J. Appl. Phys.* **78**, 5959 (1995).

⁴K. D. Mackenzie, J. R. Eggert, D. L. Leopold, Y. M. Lin, and W. Paul, *Phys. Rev. B* **31**, 2198 (1985).

⁵A. Skunanich, A. Frova, and N. M. Amer, *Solid State Commun.* **54**, 497 (1985).

⁶S. Aljishi, Z. E. Smith, D. Slobodin, J. Kolodzey, V. Chuwarz, and S. Wagner, in *Materials Issues in Amorphous-Semiconductor Technology*, edited by D. Adler, Y. Hamakawa, and A. Madan, MRS Symposia Proceedings No. 70 (Materials Research Society, Pittsburgh, 1986), p. 269.

⁷M. Fabre, A. Shah, J. Hubin, E. Bustarret, M. A. Hachicha, and S. Basrour, *J. Non-Cryst. Solids* **137/138**, 335 (1991).

⁸G. Schumm, E. Lotter, and G. H. Bauer, *Appl. Phys. Lett.* **60**, 3262 (1992).

⁹M. J. Powell and S. C. Deane, *Phys. Rev. B* **48**, 10 815 (1993).

¹⁰G. Schumm, *Phys. Rev. B* **49**, 2427 (1994).

¹¹T. Shimizu, H. Kidoh, A. Marimoto, and M. Kumeda, *Jpn. J. Appl. Phys.* **28**, 586 (1989).

¹²H. M. Branz, *Phys. Rev. B* **41**, 7887 (1990).

¹³M. Brandt, A. Asano, and M. Stutzmann, in *Amorphous Silicon Technology—1993*, edited by E. A. Schiff *et al.*, MRS Symposia Proceedings No. 297 (Materials Research Society, Pittsburgh, 1993), p. 201.

¹⁴J.-K. Lee and E. A. Schiff, *Phys. Rev. Lett.* **68**, 2972 (1992).

¹⁵M. Vanecek, J. Kocka, J. Stuchlik, and A. Triska, *Solid State Commun.* **39**, 1199 (1981).

¹⁶Z. E. Smith, V. Chu, K. Shepard, S. Aljishi, D. Slobodin, J. Kolodzey, S. Wagner, and T. L. Chu, *Appl. Phys. Lett.* **50**, 1521 (1987).

¹⁷P. Stradins, H. Fritzsche, and M. Tran, in *Advanced Metallization for Devices and Circuits—Science, Technology, and Manufactur-*

ability, edited by S. P. Murarka *et al.*, MRS Symposia Proceedings No. 337 (Materials Research Society, Pittsburgh, 1994), p. 467.

¹⁸J. Kocka, M. Vanecek, and F. Schauer, *J. Non-Cryst. Solids* **97/98**, 715 (1987).

¹⁹I. Sakata, M. Yamanaka, S. Numase, and Y. Hayashi, *J. Appl. Phys.* **71**, 4344 (1992).

²⁰M. Günes, C. R. Wronski, and T. J. McMahon, *J. Appl. Phys.* **76**, 2260 (1994).

²¹K. Pierz, H. Mell, and J. Terukov, *J. Non-Cryst. Solids* **77/78**, 547 (1988).

²²G. Amato, F. Giorgis, and R. Spagnolo, *J. Appl. Phys.* **71**, 3479 (1992).

²³P. Jensen, *Solid State Commun.* **76**, 1301 (1990).

²⁴R. Swanepoel, *J. Phys. E* **16**, 1214 (1983).

²⁵K. Seeger, in *Semiconductor Physics*, edited by M. Cardona and H.-J. Queisser, *Solid-State Sciences Vol. 40* (Springer, Berlin, 1985), p. 387.

²⁶D. Ritter and K. Weiser, *Opt. Commun.* **57**, 336 (1986).

²⁷H. Dersch, J. Stuke, and J. Beichler, *Appl. Phys. Lett.* **38**, 456 (1980).

²⁸M. Stutzmann, W. B. Jackson, and C. C. Tsai, *Phys. Rev. B* **32**, 23 (1985).

²⁹P. Tzanetakis, N. Kopidakis, M. Androulidaki, C. Kalpouzos, P. Stradins, and H. Fritzsche, in *Amorphous Silicon Technology—1995*, edited by M. Hack *et al.*, MRS Symposia Proceedings No. 377 (Materials Research Society, Pittsburgh, 1995), p. 245.

³⁰T. Tiedje, B. Abeles, and J. M. Cebulka, *Solid State Commun.* **47**, 493 (1983).

³¹N. Wyrsh, F. Finger, T. J. McMahon, and M. Vanecek, *J. Non-Cryst. Solids* **137/138**, 347 (1991).

³²F. Siebke and H. Stiebig (unpublished).

³³M. Vanecek, J. Kocka, J. Stuchlik, Z. Kosizek, O. Stika, and A. Triska, *Solar Energy Mater.* **8**, 411 (1983).

³⁴J. M. Marshall, W. Pickin, A. R. Hepburn, C. Main, and R. Brüggeman, *J. Non-Cryst. Solids* **137&138**, 343 (1991).

³⁵P. Sladek, Y. Bouizem, M. L. Theye, and Roca i Cabarrocas (unpublished).

³⁶D. K. Biegelsen, R. A. Street, and R. L. Weisfield, *J. Non-Cryst. Solids* **66**, 139 (1984).

- ³⁷R. A. Street, M. Hack, and W. B. Jackson, *Phys. Rev. B* **37**, 4209 (1988).
- ³⁸R. A. Street and K. Winer, *Phys. Rev. B* **40**, 6236 (1989).
- ³⁹K. Winer, *Phys. Rev. B* **41**, 12 150 (1990).
- ⁴⁰H. M. Branz and M. Silver, *Phys. Rev. B* **42**, 7420 (1990).
- ⁴¹C. M. Fortman, R. M. Dawson, H. Y. Liu, and C. R. Wronski, *J. Appl. Phys.* **76**, 768 (1994).
- ⁴²H. Liu, C. T. Malone, C. M. Fortmann, and C. R. Wronski, in *Advanced Metallization for Devices and Circuits—Science, Technology, and Manufacturability* (Ref. 17), p. 687.
- ⁴³H. Dersch, J. Stuke, and J. Beichler, *Appl. Phys. Lett.* **38**, 6 (1981).